Electronic Supplementary Material (ESI) for Physical Chemistry Chemical Physics.

A Coarse-Grain Force Field Based on Quantum Mechanics (CGq FF) for Molecular Dynamics Simulation of Poly(Ethylene Glycol)-block-Poly(ε-Caprolactone) (PEG-*b*-PCL) Micelles

Maryam S. Sadeghi,[†‡] **M. R. Moghbeli,**[1*] [†‡] **William A. Goddard III**[*‡]

[†‡] *Smart Polymers and Nanocomposites Research Group, School of Chemical Engineering, Iran University of Science and Technology, Tehran 16846–13114, Iran.*

[‡] *Materials and Process Simulation Center (MSC), California Institute of Technology, Pasadena, California 91125. USA*

[1*] Corresponding author email address: W. A. Goddard III (wag@caltech.edu), M. R. Moghbeli (mr_moghbeli@iust.ac.ir)

ORCID wag:0000-0003-0097-5716

SI.1. Water Model: Each MARTINI water bead (P4) represents 4 water molecules. A possible problem with pure MARTINI water is that rapid and irreversible [1] freezing has been reported at temperatures between 280 and 300 K. To avoid freezing, 10% of the water beads were replaced with antifreeze agents, denoted by BP4 MARTINI bead, for all simulations. To disturb the lattice packing of the solvent particles, a 21% radius increase is applied to the BP4 beads compared to the P4 beads for all simulations. No nucleation was observed in any of the PEG/water simulations carried out for this study.

To test our water model, 1071 MARTINI water beads were added to a box of 5 × 5 × 5 nm^3. The system was relaxed and then subjected to 10 ns equilibration, followed by equilibration for 100 ns using the isothermal-isobaric ensemble with a velocity rescale (V-rescale) thermostat using a coupling constant of 1 ps to maintain the temperature at 300 K. These simulations reproduced the water structure well with a density of 1.02 g/cm^3 and a cumulative number of 13.7 at the first minimum of the RDF. To test the liquid–vapour equilibrium, the water molecules were inserted in a 5 × 5 × 20 nm^3 slab, and then equilibrated for 10 ns followed by a 100 ns production run. The liquid–vapour simulations were all carried out in the canonical ensemble. We performed the liquid–vapour simulations of our water model using a simple cutoff with rc=2.45 nm, approximately half of the box width. The simulation results represented a surface tension of the MARTINI water model equal to 62.5 mN/m at 300 K, in reasonable agreement with the experimental value of 71.7 mN/m [2]. Based on recent studies, bond flexibility, long range electrostatic interactions, such simulation parameters as Lennard-Jones (LJ) cutoff distance, and simulation timescale, may play an important role in determining the predicted surface tension [3].

SI.2. Target Atomistic Force Field: Atomistic simulations were performed using different all-atom (AA) and united-atom (UA) force field (FF) parameterizations commonly applied to simulation of biological molecules. Two observables, radius of gyration and end to end distance that are two critical measures of polymer geometry and intrinsic properties such as flexibility were calculated, using each tested FF parameters and for each single chain of CG-PEG_9 and CG-PCL_{10} systems and compared with experimental data (Tables SI-1 and SI-2).

Table SI-1. Simulated and Experimental Structural Properties of diluted PEG_9: R_g Radius of Gyration and $\langle h^2\rangle^{\frac{1}{2}}$ Root Mean Squared End-to-End Distance, $and\ \rho$ Density of Dilute System

	$R_g(Å)$	$\langle h^2\rangle^{\frac{1}{2}}(Å)$	$\rho(g.cm^{-3})$
CG	5.733	14.300	1.0129
AA-CHARMM36	5.906	14.176	1.015
AA-CHARMM27	8.275	24. 790	0.998
AA-OPLS/CM1A	5.262	12.240	0.999

AA-Gromos54a7	5.903	14.002	0.999
Experiment*	5.600	15.500	1.002

Table SI-1 Among the tested AA and UA FFs, the CHARMM36 reproduces the structural properties of the single chain PEG₉ very well, thus we use this AA FF as our target FF for reproduction of the CG valence parameters (AA-CHARMM27 FF, overestimates the interactions between the ether units and water sites, resulting in higher values of radius of gyration, end-to-end distance, and diffusion coefficient).

Figures SI-1 and SI-2 compare the probability distribution of CG and AA/UA end to end distances and average of radius of gyration of PEG₉ (the results for CHARMM27 is not presented).

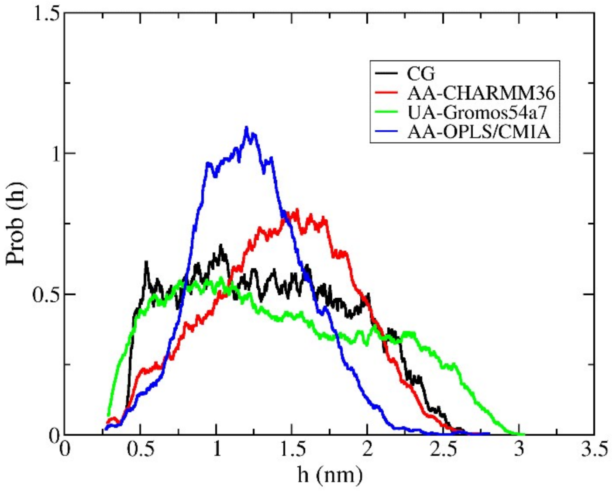

Figure SI-1. Probability distribution of end to end distances of CG PEG₉ (black) with the AA-CHARMM36 (red), UA-GROMACS541a7 (green) and AA-OPLS/CM1A (blue) FFs.

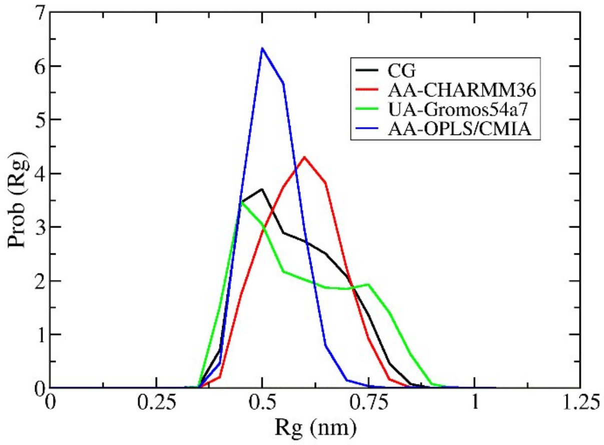

(a)

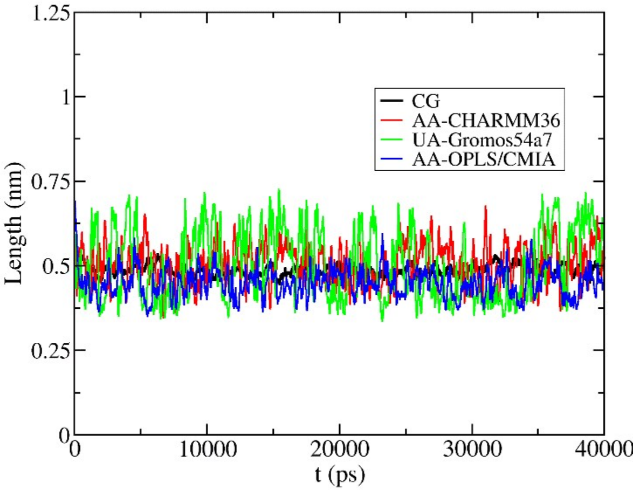

(b)

Figure SI-2. (a) Probability distribution and **(b)** average radius of gyration of CG-PEG$_9$ (black) compared to the AA-CHARMM36 (red), UA-GROMACS541a7 (green) and AA-OPLS/CM1A (blue) FFs.

The calculated radius of gyration and end-to-end distance for the single chain CG – PCL$_{10}$ system is compared with the tested AA and UA potentials in Table SI-2.

Table SI-2. Simulated and Experimental Structural Properties of diluted PCL$_{10}$: R_g Radius of Gyration and $\langle h^2\rangle^{\frac{1}{2}}$ Root Mean Squared End-to-End Distance.

	CG	AA-CHARMM27	AA-OPLS/CM1A	UA-Gromos54a7	AA-OPLS (Pasquale et al)*
R_g(Å)	6.643	7.060	6.790	6.380	6.400
$\langle h^2\rangle^{\frac{1}{2}}$(Å)	13.799	14.574	13.002	12.010	13.400

* All-atom simulation results of Di Pasquale et al [4].

The AA OPLS/CMIA FF parameters is taken to reproduce the CG valence parameters for this polymer. The time averaged principle moments of gyration tensor were also calculated for CG – PCL$_{10}$ system and compared to the AA and UA simulations (Table SI-3).

Table SI-3. Time Averaged Principle Moments of Gyration Tensor (λ) of diluted CG and AA / UA PCL$_{10}$

	λ_1(Å)	λ_2(Å)	λ_3(Å)
CG	5.395	5.385	5.400
AA-CHARMM27	5.774	5.610	5.770
AA- OPLS/CM1A	5.831	5.559	5.373
UA-Gromos54a7	5.476	5.078	5.205

The probability distribution of end-to-end distances and average radius of gyration for the CG- and AA/UA models of PCL$_{10}$ are compared in Figures SI-3 and SI-4.

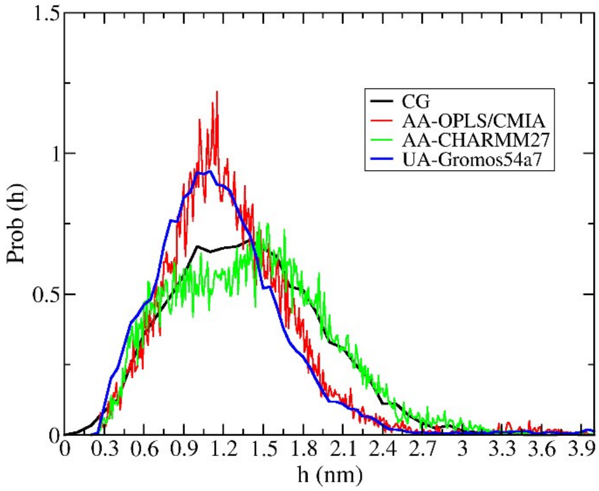

Figure SI-3. Probability distribution of end-to-end distances of CG PCL_{10} and 3 tested AA/UA FFs

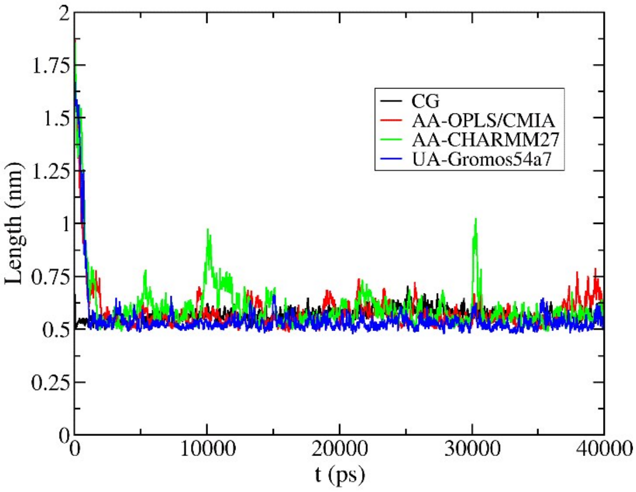

Figure SI-4. Average radius of gyration of CG PCL_{10} and 3 tested AA/UA FFs.

SI.3. Probability Distributions of Valence Terms: Each coarse-grained bead in our model is defined as the center of mass of particles in the atomistic structure. The corresponding valence distribution functions are characterized by Gaussian distributions where the height to width of the functions determine the strength of the harmonic bond and angle and the location of the peaks give the equilibrium distance and angles (see Figure. SI-5 and Figure SI-6). AA-CHARMM36 and AA-OPLS/CMIA FF are taken as the target FFs for PEG and PCL, respectively. As shown in Figures SI-5 and SI-6, the CG distribution functions show very good agreement with the target AA distribution functions. Figure SI-6 shows that the AA angle distributions have double peaks (bimodal), while the CG distributions are unimodal for PCL. The underlying reason for these two different distributions is that the carbon-oxygen double bond in the backbone structure of PCL is very rigid in torsion, while the carbon-carbon single bonds can easily flip from one torsional state to another.

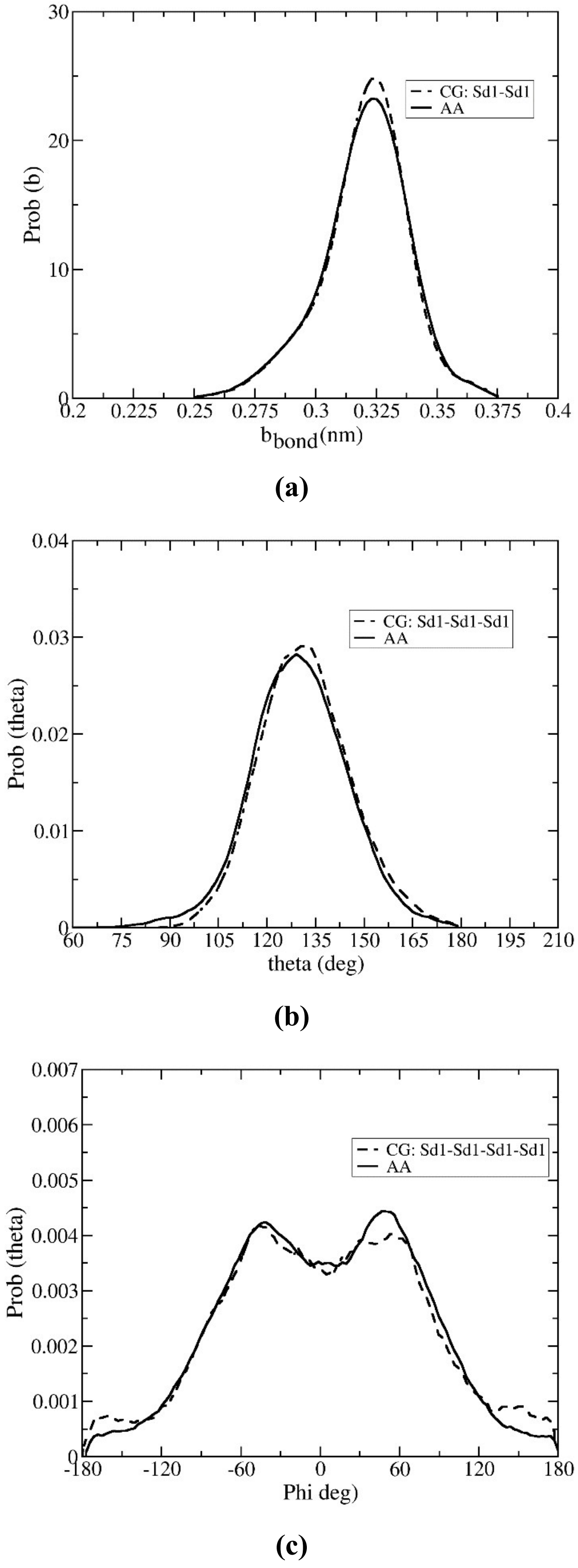

Figure SI-5. Probability distributions of **(a)** core bonds Sd1-Sd1, **(b)** core angles Sd1-Sd1-Sd1, and **(c)** core dihedrals Sd1-Sd1-Sd1 of PEG_9 from all-atom (solid line) and CG (dashed line).

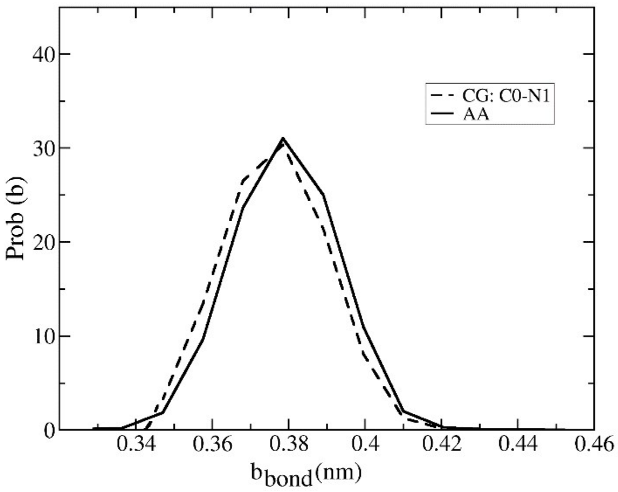
Prob (b)
0
10
20
30
40
0.34
0.36
0.38
0.4
0.42
0.44
0.46
b_{bond}(nm)
CG: C0-N1
AA

(a)

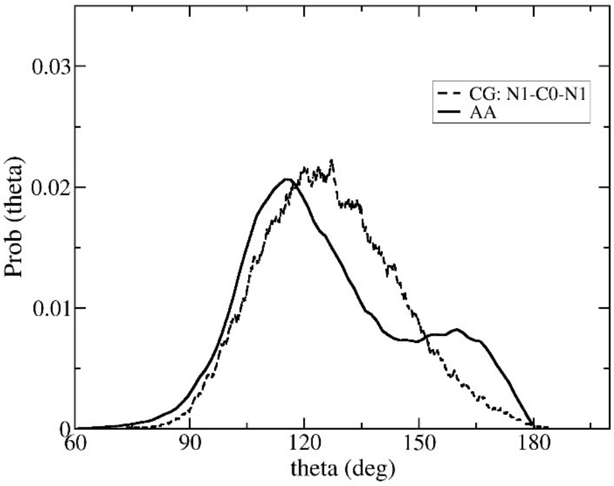
Prob (theta)
0
0.01
0.02
0.03
60
90
120
150
180
theta (deg)
CG: N1-C0-N1
AA

(b)

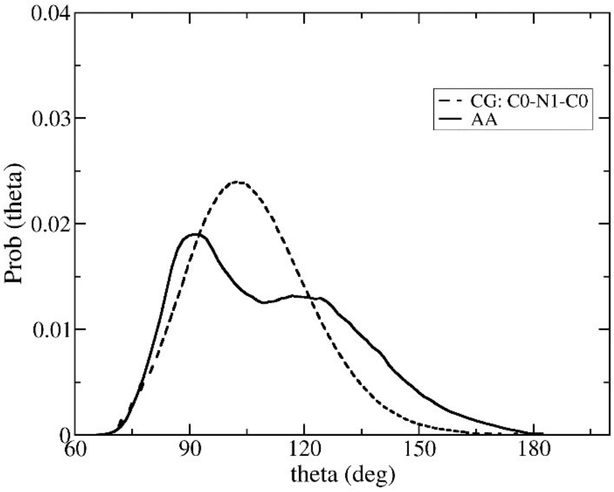
Prob (theta)
0
0.01
0.02
0.03
0.04
60
90
120
150
180
theta (deg)
CG: C0-N1-C0
AA

(c)

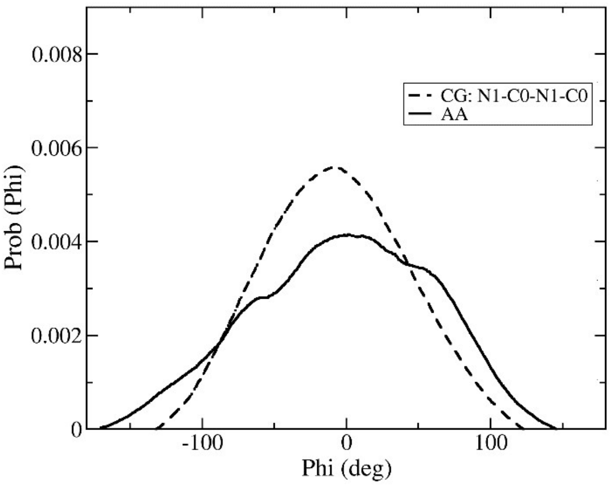

(d)

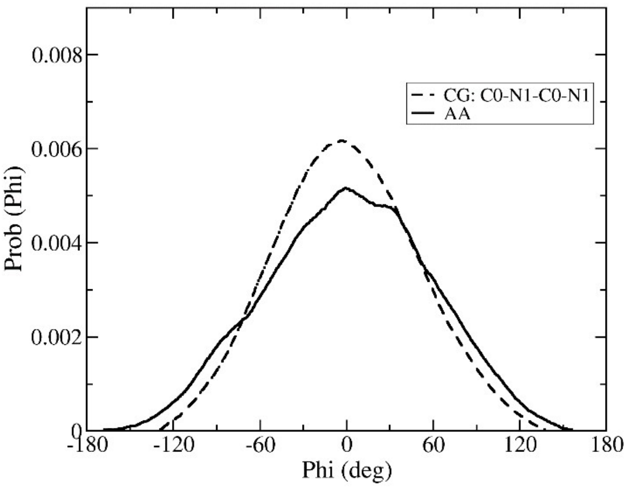

(e)

Figure SI-6. Probability distributions of **(a)** core bonds C0-N1, **(b)** core angles N1-C0-N1, **(c)** core angles C0-N1-C0, **(d)** core dihedrals N1-C0-N1-C0 and **(e)** core dihedrals C0-N1-C0-N1 of PCL_{10} from all-atom (solid line) and CG (dashed line).

References

(1) Marrink, S. J.; Risselada, H. J.; Yefimov, S.; Tieleman D. P.; de Vries, A. H. The MARTINI Force Field: Coarse Grained Model for Biomolecular Simulations. J. Phys. Chem. B, **2007**, 111, 7812-7824.

(2) Vargaftik, N. B.; Volkov, L. D. International Table of the Surface Tension of Water. J. Phys. Chem. Ref. Data, **1983**, 12, 817-820

(3) Yuet, P. K.; Blankschtein, D. Molecular Dynamics Simulation Study of Water Surfaces: Comparison of Flexible Water Models. J. Phys. Chem, B, **2010**, 114: 13786–13795.

(4) Di Pasquale, N., Marchisio, D.L., Barresi, A.A., Carbone, P., Solvent Structuring and Its Effect on the Polymer Structure and Processability: The Case of Water–Acetone Polyε-caprolactone Mixtures. J. Phys. Chem. B, **2014**, 118, 13258–13267.